Clim Dyn (2018) 50:1193–1207
DOI 10.1007/s00382-017-3672-3

# Effect of the atmospheric quasi-biweekly oscillation on the vortices moving off the Tibetan Plateau

**Lun Li[1] · Renhe Zhang[2,3] · Min Wen[1] · Junmei Lü[1]**

Received: 22 October 2016 / Accepted: 10 March 2017 / Published online: 5 April 2017


**Abstract** In the present study, the relationship between the atmospheric quasi-biweekly oscillation (QBWO) and Tibetan Plateau vortices (TPVs) moving off the Tibetan Plateau was investigated based on the radiosonde and reanalysis data. It is found that the number of TPVs moving off the Tibetan Plateau (moving-off TPVs) has the distinct feature of the 10–20-day QBWO. 77% of the moving-off TPVs occur in the positive phases of the 10–20-day filtered 500 hPa vorticity over eastern Tibetan Plateau. Besides, distributions of the zonal and meridional components of E-vectors coincide well with the trajectories of TPVs, indicating the moving-off TPVs are well related with the propagation of the QBWO energy. The atmospheric circulations and related thermodynamic fields are discussed to reveal the mechanism of the effect of 10–20-day QBWO on the moving-off TPVs. It is found that the atmospheric circulations and heating fields of 10–20-day QBWO have major impact on the moving-off TPVs. In positive QBWO phases, at 500 hPa over eastern Tibetan Plateau, there appear negative geopotential height anomalies and anomalous cyclonic wind shear; the anomalous jet stream and positive geopotential heights at 200 hPa lying over the northeast of the Tibetan Plateau stretch eastward gradually, benefiting for the upper level divergence and ascending motion. The condensation latent heat is released and shifts eastward with the heating centers located at 400 hPa, which depresses the isobaric surface at 500 hPa. All these conditions are in favor of the maintenance and eastward movement of TPVs in the positive QBWO phases.

**Keywords** Tibetan Plateau vortices · Quasi-biweekly oscillation · Large scale circulations · Condensation latent heat

## 1 Introduction

In boreal summer, the low-level cyclonic vortices forming over the Tibetan Plateau (hereafter referred to as TPVs) are the major mesoscale rain-producing system over the Tibetan Plateau (Ye and Gao 1979; Lhasa Workgroup for Tibetan Plateau Meteorology Research 1981). Most of TPVs originate over the central-western plateau, and decay over eastern Tibetan Plateau, especially over the sloping terrain at the eastern edge of the Tibetan Plateau. Some of them can maintain for a long time and move eastward out of the plateau (Ye and Gao 1979; Qiao and Zhang 1994; Li 2002; Wang et al. 2009; Li et al. 2014a; Yu et al. 2016). The TPVs moving off the plateau often trigger heavy rainfall to the east of the Tibetan Plateau, and even give rise to disastrous weather events over eastern China (Ye and Gao 1979; Qiao and Zhang 1994; Li 2002). The typical spatial scale of TPVs is about 400–800 km in horizontal and 2–3 km in vertical. The cyclonic circulation associated with TPVs is primarily confined to the lower-middle troposphere, with positive vorticity reaching maximum at 500 hPa and disappearing above 400 hPa (Ye and Gao 1979; Lhasa Workgroup for Tibetan Plateau Meteorology Research 1981; Luo 1992; Luo et al. 1994).

✉ Renhe Zhang
rhzhang@fudan.edu.cn

[1] State Key Laboratory of Severe Weather, Chinese Academy of Meteorological Sciences, Beijing, China

[2] Institute of Atmospheric Sciences, Fudan University, No. 220 Handan Road, Shanghai 200433, China

[3] CAS Center for Excellence in Tibetan Plateau Earth Sciences, Beijing, China

The circulations benefiting the eastward movement of TPVs have been revealed in the previous studies. It is pointed out that the divergence on the upper-level is a dominant factor in the eastward movement of TPVs (Liu and Fu 1985), and the eastward movement is associated with the eastward moving of upper-level westerly jet stream and the eastward stretching of South Asia high (Yu et al. 2007). At 500 hPa, the eastward movement of TPVs is accompanied by the northward shifting of the monsoon trough over Bay of Bengal, westward extending of western North Pacific subtropical high, and active shear lines over eastern Tibetan Plateau (Guo 1986; Gao and Yu 2007; Gu et al. 2010). Liu and Fu (1985) pointed out that three types of TPVs, lying behind a ridge, in front of a westerly trough, and on a shear line, could move out of the plateau. The convergence to the east of TPVs at 500 hPa between the northwesterly winds invading from the north of the Tibetan Plateau and southwesterly winds from the Bay of Bengal is a prominent factor controlling the eastward moving of TPVs (Li et al. 2011, 2014a). The water vapor is another important factor affecting the eastward movement of TPVs. The TPVs move eastward when the water vapor vortex at the middle-upper troposphere is located over the east of TPVs (Yu 2002).

A lot of studies have found that the initiation, development and eastward movement of TPVs are affected by the thermodynamic factors, among which the diabatic heating would be the leading factor. It is pointed out that the sensible heating exerts a major effect on the formation of the vortices, while the condensation latent heat is most important during their developing phase (Lhasa workgroup for Tibetan Plateau meteorology research 1981; Dell'Osso and Chen 1986; Shen et al. 1986a, b; Wang 1987; Li and Zhao 2002). The diurnal variation of TPVs was investigated by Li et al. (2014b), and the condensation latent heat is emphasized as the dominant factor in the initiation process. Ding and Lu (1990) used a five-layer primitive equation model to simulate the eastward movement of a vortex over the Tibetan Plateau. They suggested that the diabatic factors, such as radiation and large-scale condensation latent heat, might only affect the intensity of the vortex. Luo et al. (1991) found that the genesis, development and decay of the plateau vortices are closely interrelated with variations of the atmospheric heat field. The numerical simulation of three vortices by Chen et al. (1996) showed that their disappearances in the sloping terrain of the eastern Tibetan Plateau might be owe to the weakening of the surface heating. Li et al. (2011, 2014a) pointed out that the atmospheric heat source not only affects the intensity of the vortex, but also influences its eastward movement. Some studies indicated that the generation of TPVs has obviously active and suppressed periods (Luo et al. 1994), and the intraseasonal oscillation (ISO) has close relationship with the occurrence of TPVs. Sun and Chen (1994) revealed that the active center of the 30–50-day filtered low frequency system over the Tibetan Plateau matches the generation center of TPVs. Zhang et al. (2014) pointed out that the occurrence of TPVs is mainly modulated by the 10–30-day ISO.

As mentioned above, previous studies mainly investigated the effect of circulation and diabatic heating on the initiation and eastward movement of TPVs, and demonstrated the close relationship between the ISO and the occurrence of TPVs. However, it is unclear if the eastward movement of TPVs is associated with ISO and what is the effect of ISO on the eastward-moving TPVs. Considering the important effect of the TPVs moving off the Tibetan Plateau (hereafter referred to as moving-off TPVs) on the rainfall to the east of the Tibetan Plateau, the research on the effect of ISO on the eastward movement of TPVs is urgently needed for understanding not only the moving-off TPVs themselves, but also the rainfall variability in eastern China. Therefore, the effect of ISO on the moving-off TPVs is investigated in the present study. The data and method utilized in this work is introduced in Sect. 2. The relationship between ISO and the moving-off TPVs are discussed in Sect. 3. In Sect. 4, we analyze the large-scale circulation and the related physical fields associated with ISO to illustrate the physical processes by which ISO affects the moving-off TPVs. Summary and discussion are given in Sect. 5.

## 2 Data and method

### 2.1 Data and definition of TPVs

The data used in the present study include the daily reanalysis data during May–August of 1998–2012 derived from the National Centers for Environmental Prediction/National Center for Atmospheric Research (NCEP/NCAR), with global coverage and 2.5° × 2.5° resolution (Kalnay et al. 1996), and 500 hPa winds from radiosonde data observed twice a day over the Tibetan Plateau, derived from the National Meteorological Information Center (NMIC) of the China Meteorological Administration (CMA) in the same period. A band-pass filter method of Lanczos (Duchon 1979) is applied to the daily data to extract the intraseasonal signals. Zhou and Zhang (2009) compared the NCEP/NCAR reanalysis with observations over the Tibetan Plateau. They found that the NCEP/NCAR reanalysis data are reasonable in reflecting the observed atmosphere over the Tibetan Plateau.

A Tibetan Plateau vortex (TPV) is defined as a low which forms over the Tibetan Plateau with closed contour lines or cyclonic winds at three observation stations at 500 hPa (Lhasa Workgroup for Tibetan Plateau Meteorology Research 1981). In choosing the TPVs we referred to the *Yearbook of*

*Tibetan Plateau Vortex and Shear Line* accomplished by the Institute of Plateau Meteorology, CMA, which started from 1998 and ended in 2012. In the present study, a moving-off TPV is defined as a TPV moving eastward and shift out of the plateau region where the elevation is over 3000 m. In addition, a moving-off TPV should generate over the main body of the Tibetan Plateau and span over 24 h.

### 2.2 E vector

*E* vector (***E***) was defined by Hoskins et al. (1983), which can be used to diagnose the horizontal structure and propagation feature of the low frequency wave energy (Xu and He 1993). The calculation formula of *E* vector is

$$\mathbf{E} = \left(\overline{v'^2 - u'^2}, \overline{-u'v'}\right) \tag{1}$$

where $\overline{v'^2 - u'^2}$ and $\overline{-u'v'}$ represent the components in $x$ and $y$ directions, respectively. $u'$ and $v'$ are the bandpass filtered zonal and meridional winds, respectively. Bars signify a time average.

### 2.3 Atmospheric apparent heat source and apparent moisture sink

To investigate the effect of the diabatic heating in the eastward moving process of TPVs, the atmospheric apparent heat source ($Q_1$) and the apparent moisture sink ($Q_2$) are calculated based on the atmospheric thermodynamic equation and the moisture equation, respectively. The equations used are as follows (Yanai et al. 1973):

$$Q1 = cp\left(\frac{\partial T}{\partial t} + \mathbf{V}\cdot\nabla T + \omega\left(\frac{P}{P0}\right)^{\kappa}\frac{\partial\theta}{\partial p}\right), \tag{2}$$

$$Q2 = -L\left(\frac{\partial q}{\partial t} + \mathbf{V}\cdot\nabla q + \omega\frac{\partial q}{\partial p}\right), \tag{3}$$

where $T$ is the temperature, $\boldsymbol{V}$ and $\omega$ denote the horizontal wind vector and the vertical wind component in pressure coordinates, respectively. $P_0$ is the pressure of 1000 hPa. $c_p$ represents the specific heat at constant pressure, and $\kappa \approx 0.286$. $\theta$ is the potential temperature. $L = 2.5\times10^6$ J kg$^{-1}$, denoting the latent heat of condensation, and $q$ is the specific humidity.

### 2.4 Water vapor flux

The water vapor condition has close relationship with the condensation latent heat, thus the vertically integrated water vapor flux is calculated using the following equation (Rasmusson 1968).

$$\mathbf{A} = \frac{1}{g}\int_{Pu}^{Ps} q\mathbf{V}\mathrm{d}p \tag{4}$$

***A*** and ***V*** denote the water vapor flux and the horizontal wind vector, respectively. $P_s$ is the pressure at the ground, and $P_u$ is the pressure of upper-level where the water vapor flux divergence is negligibly small, usually $P_u$=300 hPa. $q$ represents the specific humidity.

## 3 Relationship between QBWO and the moving-off TPVs

In order to investigate the moving-off TPVs, an area 95°–105°E, 30°–40°N in eastern Tibetan Plateau (hereafter referred to as ETP) is chosen and the power spectrum of 500 hPa vorticity averaged over ETP is calculated because of the close relationship between 500 hPa vorticity and TPVs. The ratio of the power spectrum and the red noise spectrum at $\alpha = 0.05$ significance level is shown in Fig. 1, in which values greater than 1.0 indicate the periods exceeding 95% confidence level. It can be seen that before 2003, both the intraseasonal oscillations in the time scales around 20 and 10 days were statistically significant, and, afterwards the significant intraseasonal oscillation mainly concentrated within 10–20 days. Therefore, in the intraseasonal timescale, the quasi-biweekly oscillation (QBWO) in about 10–20-day is statistically significant spanning from 1998 to 2012. It is obvious that the variation of 500 hPa vorticity in ETP has the clear feature of QBWO.

By applying the Lanczos bandpass filter, the10–20-day QBWO of 500 hPa vorticity averaged over ETP is extracted. Based on the standardized QBWO, 65 life cycles with amplitude greater than 1.0 are selected to compose 8 QBWO phases. As shown in Fig. 2, the composite for the life cycle of the 10–20-day QBWO is separated into eight phases, in which phases 1–4 are positive phases, and 5–8 negative phases. To show the evolution of the10–20-day QBWO of 500 hPa vorticity averaged over the Tibetan Plateau, in Fig. 3 we depict the phase-longitudinal cross-section for the QBWO of vorticity averaged in the latitudes 30°N–37.5°N where the Tibetan Plateau is located. It can be seen that to the east of 90°E, as the phase increases, the vorticity has a clear feature of moving eastward. Over the ETP area (95°–105°E, 30°–40°N), the strongest and weakest phases of the QBWO are in phases 3 and 7, respectively.

To check the relations of the moving-off TPVs with the QBWO, for the 91 moving-off TPVs during May–August of 1998–2012, there are 70 occurred in positive phases and 21 in negative phases. The ratio for the numbers of the moving-off TPVs in positive phases to the total reaches 77%, indicating the moving-off TPVs mainly exist in the positive phases of QBWO. In Fig. 4 the trajectories of the moving-off TPVs and composites of the 10–20-day QBWO of 500 hPa vorticity in positive and negative phases are shown. It can be seen the moving-off TPVs are mainly

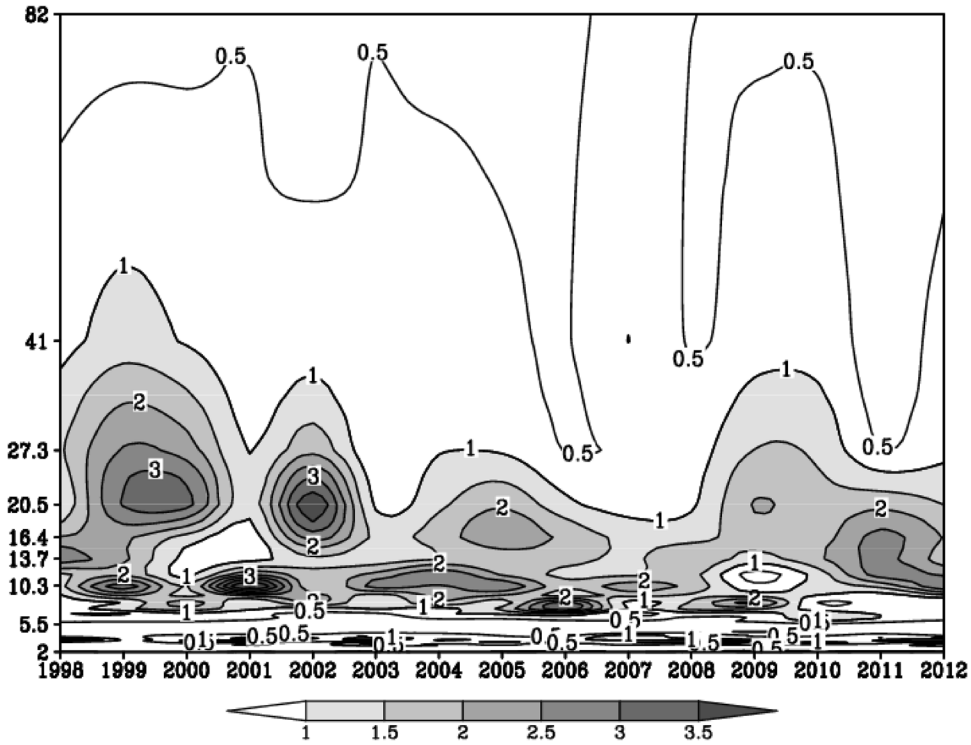


**Fig. 1** Ratios of the power spectrum of 500 hPa vorticity averaged over 95°–105°E, 30°–40°N in eastern Tibetan Plateau and the red noise spectrum at $\alpha = 0.05$ significance level. Values greater than 1 indicate the periods exceeding 95% confidence level (*shadings*). *Y-axis* and *x-axis* denote the period (unit: day) and time (unit: year), respectively

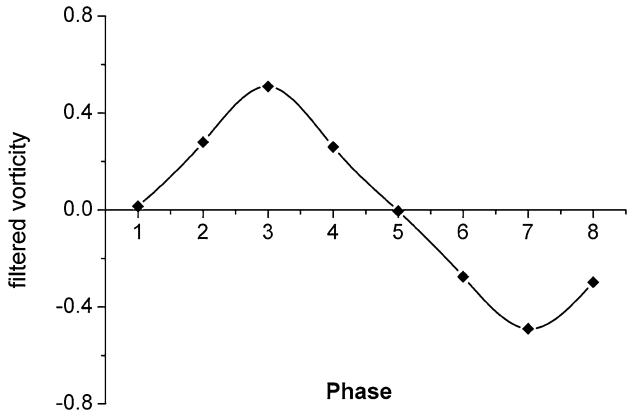


**Fig. 2** Phases for the filtered 10–20-day QBWO of 500 hPa vorticity averaged over 95°–105°E, 30°–40°N in eastern Tibetan Plateau (unit: $10^{-5}$ s$^{-1}$)

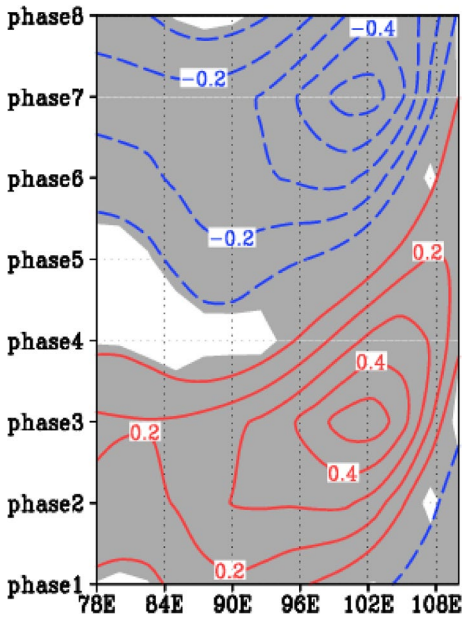


**Fig. 3** Phase-longitudinal cross-section of 10–20-day filtered vorticity at 500 hPa averaged between 30°N–37.5°N (unit: $10^{-5}$ s$^{-1}$). The shadings represent the area with statistical significance exceeding 95% confidence level

associated with the positive phase of the vorticity QBWO, while much fewer with the negative phase. To exhibit this relationship more explicitly, Fig. 5 is given to present the locations of the moving-off TPVs in the eight phases of 500 hPa vorticity QBWO separately. It can be seen that, along with the eastward propagation of 500 hPa vorticity QBWO (Fig. 3), the locations of TPVs stretch eastward from phase 1–8, indicating the eastward movement of TPVs. It is clear that the frequencies of the locations appearing in the positive phases are much higher than those in negative phases. The total numbers of locations are 323 in positive phases (from phase 1–4) but only 163 in negative phases (from phase 5–8), implying a favorable situation in positive phases for the maintenance of the moving-off TPVs.

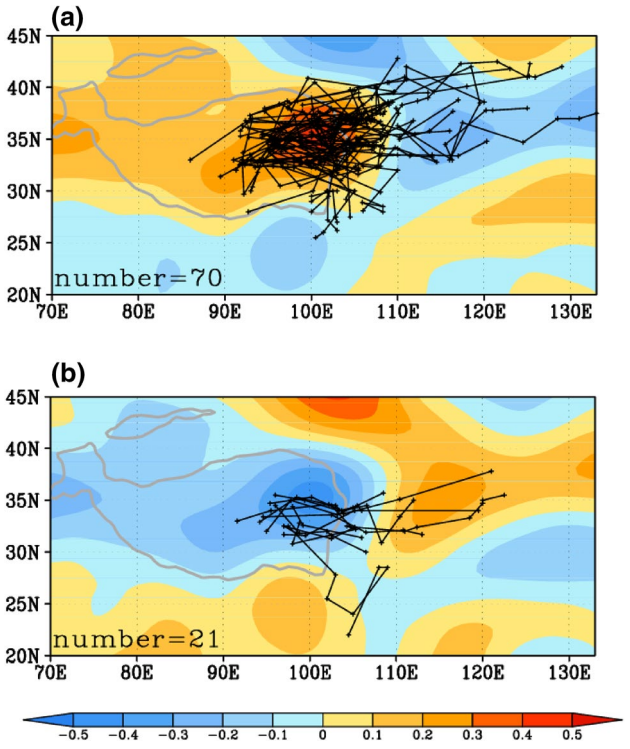


**Fig. 4** Composites of the 10–20-day filtered 500 hPa vorticity (*shadings*; unit: $10^{-5}$ $s^{-1}$) and trajectories of the moving-off TPVs in (**a**) positive and (**b**) negative phases, respectively. The *gray solid line* is the topographic contour of 3000 m

The above analyses indicate that the frequency of moving-off TPVs is modulated by the QBWO. However, although the positive phases are conducive to the occurrence of moving-off TPVs, the largest frequency obviously appears in the strongest positive phase of QBWO (phase 3). The frequency of locations in phase 3 (171) is 4.07, 2.76, and 3.56 times as high as those in phases 1 (42), 2 (62), and 4 (48), respectively. Meanwhile, although the contrast of the frequencies between the strongest positive phase (phase 3) and the strongest negative phase (phase 7) is largest, with a ratio as large as 4.07, the contrasts of other positive phases to their corresponding negative phases, nevertheless, are not so large, with the ratios of 1.20, 1.32, 1.23 between phases 1 and 5, 2 and 6, 4 and 8, respectively. Here we can see that the modulation of QBWO on the frequency of the moving-off TPVs mainly occurs in the strongest positive phase of QBWO.

In order to investigate the relationship between the propagation of the low frequency energy and the movement of TPVs, we calculated the *E* vector of the filtered 10–20-day QBWO at 500 hPa around the Tibetan Plateau region. The zonal and meridional components of *E* vectors are displayed in Fig. 6. Positive zonal component of *E* vectors appears around the east part of the Tibetan Plateau. The eastward propagation of the low frequency energy over the east part of the Tibetan Plateau is well related with the moving-off TPVs which move eastward (Fig. 6a). Meanwhile, as shown in Fig. 6b, the positive meridional component of *E* vectors to the north of about 34°N indicates that the low frequency energy propagates northward over there, while the negative one to the south of about 34°N means a southward propagation of the low frequency energy. This distribution of the meridional component of *E* vectors coincides well with the trajectories of the moving-off TPVs. The stronger positive meridional component of *E* vectors to the northeast of the Tibetan Plateau corresponds to a dominant northward movement of the moving-off TPVs to the north of about 34°N in their eastward-moving processes, but much less TPVs shift southward to the south of about 34°N because of the weaker negative meridional component to the southwest of the Tibetan Plateau. Thus, it is obvious that not only the moving-off TPVs has the feature of QBWO, but the propagation of the low frequency energy is well related with the movement of TPVs. To reveal the physical mechanisms of the 10–20-day QBWO of the moving-off TPVs, we will explore the roles played by the large-scale circulations and related physical factors in the QBWO of the moving-off TPVs in the next section.

## 4 Effect of QBWO on the moving-off TPVs

### 4.1 Large scale circulations

Figure 7 shows the composites of 10–20-day filtered 500 hPa winds and geopotential heights for eight QBWO phases. In phases 1–4, negative geopotential height anomalies occupy the Tibetan Plateau and extend eastward, which are in favor of the maintenance and eastward movement of TPVs. Meanwhile, the positive geopotential height anomalies located to the northeast of the Tibetan Plateau propagate southeastward. These two systems get stronger and reach the peaks in phase 3, benefiting for the enhancement of cyclonic wind shear over ETP. In fact, the cyclonic shear shifts eastward from phase 1 to 4, and becomes the strongest in phase 3 when the maximum numbers of the moving-off TPVs occur. In phases 5–8, positive geopotential height anomalies dominate the Tibetan Plateau, in conjunction with the negative anomalies to the northeast of the plateau, forming anticyclonic wind shear over ETP. Thus, the circulations at 500 hPa in the positive phases are in favor of the occurrence and eastward movement of TPVs. In addition, as shown in Fig. 7, in phase 1 a weak anomalous high first appears over central Asia with its center at about 55°N, 85°E. This anomalous high then strengthens and stretches southeastward in the following positive phases, enhancing the circulation over ETP. During the negative QBWO phases, same situation for an anomalous low can also be

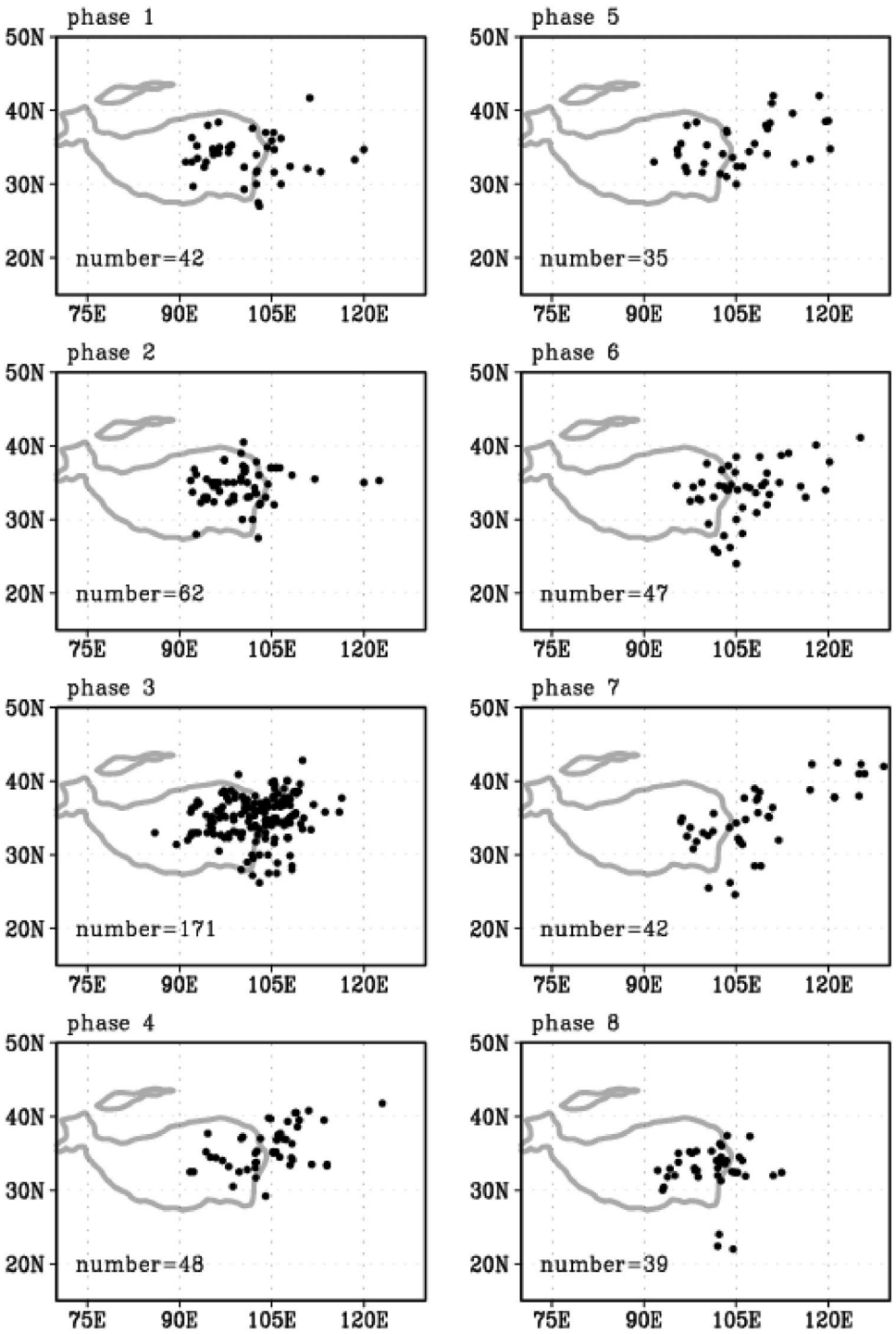


**Fig. 5** Locations of the moving-off TPVs in eight phases of 500 hPa vorticity QBWO. The *gray solid line* is the topographic contour of 3000 m

observed. These results suggest that the anomalous circulations associated with the QBWO may be traced back to the anomalous signals from higher latitudes originated around central Asia.

At 200 hPa (Fig. 8), in phases 1–4, the anomalous jet stream is located over the northeast of the Tibetan Plateau, and stretches eastward gradually. The intensity of wind speed reaches the peak in phase 3. Usually there is divergence on the right-hand side of the entrance of the jet core (Xuan et al. 2011; Jia and Yang 2013). Besides, the geopotential height anomalies increase from phase 1 to 4 over the eastern plateau and strong positive anomalies can be found over ETP in phases 3 and 4. Such situations are in favor of the upper-level divergence over ETP and strengthen the ascending motion there. In fact, the geopotential height anomalies reflect the changes of the South

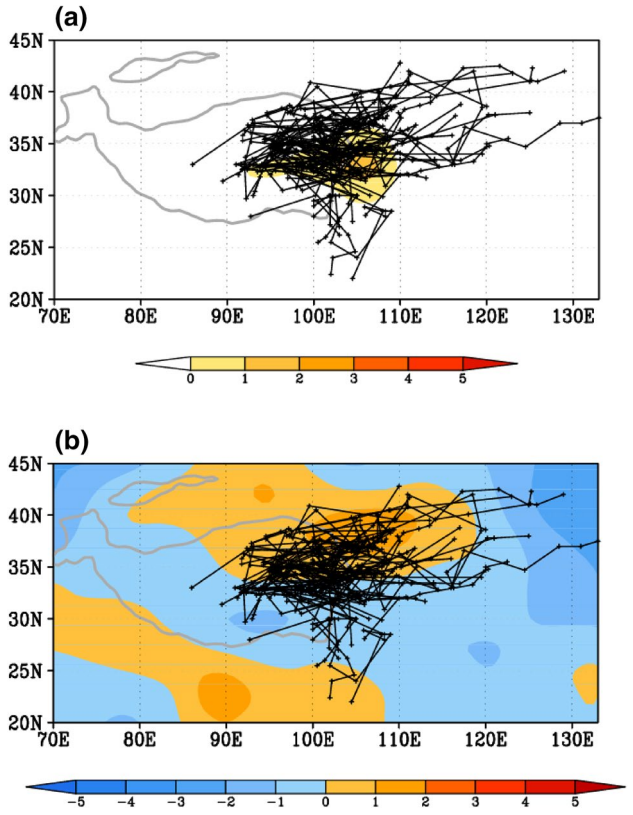


**Fig. 6** Trajectories of the moving-off TPVs (*black solid lines*) and **a** zonal and **b** meridional components of E vectors of the 10–20-day QBWO at 500 hPa (*shadings*; unit: $m^2\ s^{-2}$). The *gray solid line* is the topographic contour of 3000 m

Asian High located over the Tibetan Plateau, which is closely related with the westerly jet (Wei et al. 2017). The study by Jia and Yang (2013) also demonstrated the QBWO of the South Asian High may affect that of the upper level divergence. In negative phases (phases 5–8), the intensity of the anomalous jet stream to the northeast of the Tibetan Plateau is much weaker compared with that in positive phases (phases 1–4), and a decrease of geopotential height anomalies is found to the east of the plateau in phases 5–8 and obvious negative anomalies form over ETP in phases 7 and 8. Therefore, the circulation anomalies at upper-level in phases 1–4 are in favor of the TPVs moving off the Tibetan Plateau, but not in phases 5–8.

### 4.2 Atmospheric thermodynamic features

To discuss the atmospheric stratification features over the Tibetan Plateau, we calculate the potential pseudo-equivalent temperature ($\theta_{se}$). The height-longitude sections of the composites of 10–20-day filtered $\theta_{se}$ averaged between 30°N–40°N for eight QBWO phases are given in Fig. 9. Owing to the negligibly small specific humidity above 300 hPa and the $\theta_{se}$ above 300 hPa is nearly zero, in Fig. 9 the vertical distribution of anomalous $\theta_{se}$ is given from 1000 to 300 hPa. In positive phases, there are positive centers of $\theta_{se}$ anomalies located below 400 hPa which propagate eastward over the Tibetan Plateau, indicating eastward propagation of the unstable condition. In phase 3 the anomalous positive $\theta_{se}$ moves to ETP and its intensity reaches the maximum, implying that the strongest unstable stratification appears in this phase. At phase 5, a negative center of anomalous $\theta_{se}$ is found near 600 hPa at about 80°E, and then gets stronger and moves eastward onto the Tibetan Plateau gradually and then to ETP from phase 6 to 8, implying an unfavorable condition for the maintenance of TPVs. The positive anomalies of $\theta_{se}$ over ETP indicate a warm and humid air over there and negative anomalies a cold and dry one. In order to prove this, the water vapor transport is discussed below.

The composites of 10–20-day filtered vertical integrated water vapor flux and water vapor flux divergence are shown in Fig. 10. In positive phases, there are two water vapor convergence centers. One is along the south edge of the Tibetan Plateau, and the other stretches from the eastern plateau to about 120°E. It can be clearly seen that the water vapor transported to eastern Tibetan Plateau is mainly from the Arabian Sea (phases 1–3), suggesting that the water vapor originated from the tropical ocean may affect the QBWO around the Tibetan Plateau. The vectors of water vapor flux over the eastern plateau coincide with the cyclonic wind shear at 500 hPa in positive phases (Fig. 7), indicating the important effect of 500 hPa winds on the water vapor transportation. Therefore, the 500 hPa southerly winds transport warm and humid air from the south and the warm and humid air converges over ETP, leading to strong thermal instability in positive phases over there. On the contrary, in negative phases the northerly winds transport cold and dry air from the north to ETP and the water vapor diverges over ETP, suppressing the thermal instability over the east of the Tibetan Plateau. Meanwhile, a weakened water vapor transport from the Arabian Sea in phases 5–7 also can be observed.

Previous studies have revealed that the condensation latent heat has important effect on the evolution of TPVs (Li et al. 2011, 2014a, 2014b). Figure 11 shows the composites of 10–20-day filtered vertically integrated atmospheric apparent moisture sink ($<Q_2>$) for eight QBWO phases. Obvious eastward propagation of the heating center over the Tibetan Plateau is exhibited in phases 1–4, and the intensity of heating is much stronger in phases 2–4 than that in phase 1. The values of the $<Q_2>$ are similar to those of the atmospheric heat source ($<Q_1>$) (figure not shown), implying the condensation latent heat is the major component of the atmospheric heat source. In fact, the cyclonic shear at 500 hPa and divergence at 200 hPa in positive phases can trigger the updraft of warm and humid air over

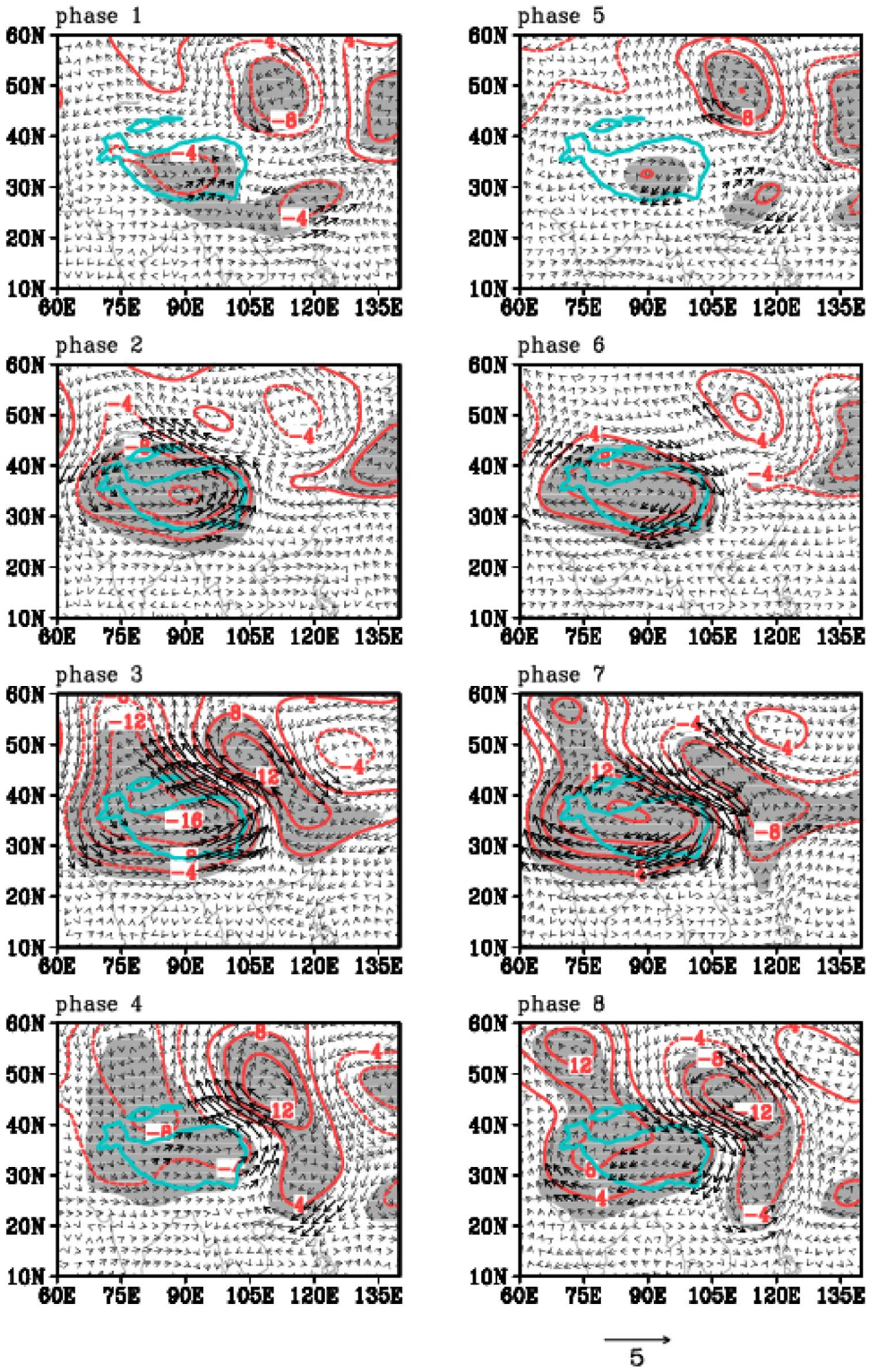


**Fig. 7** Composites of 10–20-day filtered 500 hPa winds (vectors; unit: m $s^{-1}$) and geopotential heights (*red contours*; unit: gpm) for eight phases. The geopotential heights and winds with statistical significance exceeding 95% confidence level are *shaded* and *black-colored*, respectively. The *blue solid line* is the topographic contour of 3000 m

the eastern downstream region of the plateau, and the water vapor converges there, which are favorable for more precipitation and thus the release of condensation latent heat, resulting in positive anomalies of $<Q_2>$ over there. The eastward propagation of condensation latent heat facilitates the strengthening and moving eastward of TPVs through increasing potential vorticity (PV) tendency (Li et al. 2011, 2014a). In phases 5–8, the cold and dry air transported to ETP leads to the deficiency of moisture, and thus weakens the condensation latent heat.

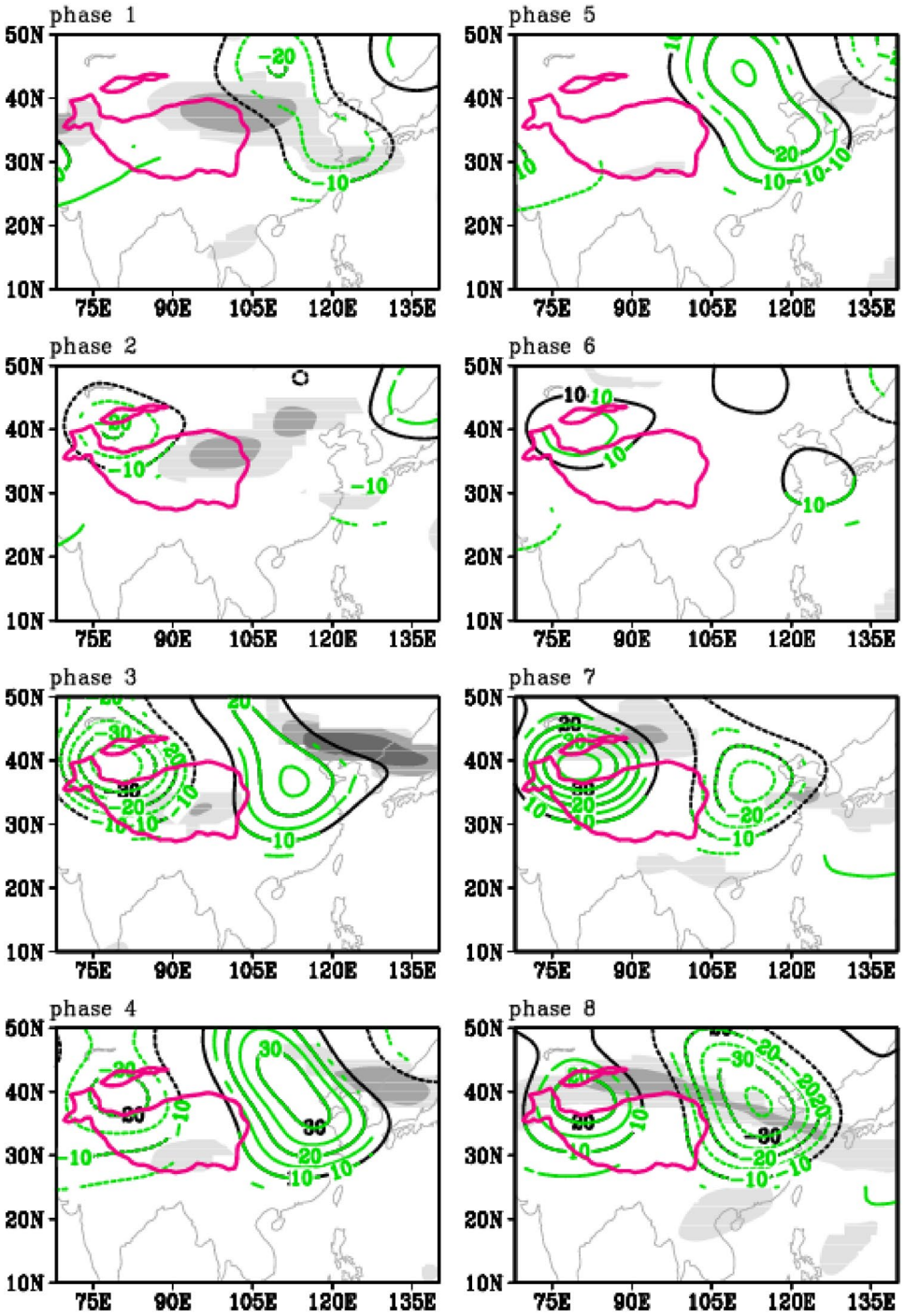


**Fig. 8** Same as Fig. 7, but for geopotential heights (*contours*; unit: gpm) and wind speeds (*shadings*; unit: m $s^{-1}$) at 200 hPa. Only the wind speeds exceeding 95% confidence level are plotted

Figure 12 exhibits the vertical cross-sections of composites of 10-20-day filtered atmospheric heat source $Q_1$ averaged between 30°N–40°N for eight QBWO phases. It can be seen that the heating centers of the atmospheric heat source $Q_1$ are located at about 400 hPa in phases 1–4. The heating can strengthen the low-level cyclonic disturbances at 500 hPa through depressing the isobaric surface in lower troposphere, benefiting for the maintenance and development of TPVs. However, the cooling anomalies in phases 5–8 can exert opposed effect on circulations, which hampers the maintenance and development of TPVs.

From the analyses above, in positive phases the eastward-moving cyclonic wind shear at 500 hPa as well as 200 hPa divergence are in favor of the ascending motion. Meanwhile, the water vapor converges over ETP, thus stronger precipitation can be induced. The condensation latent heat related to the precipitation is released and shifts eastward, with the heating centers being located at 400 hPa.

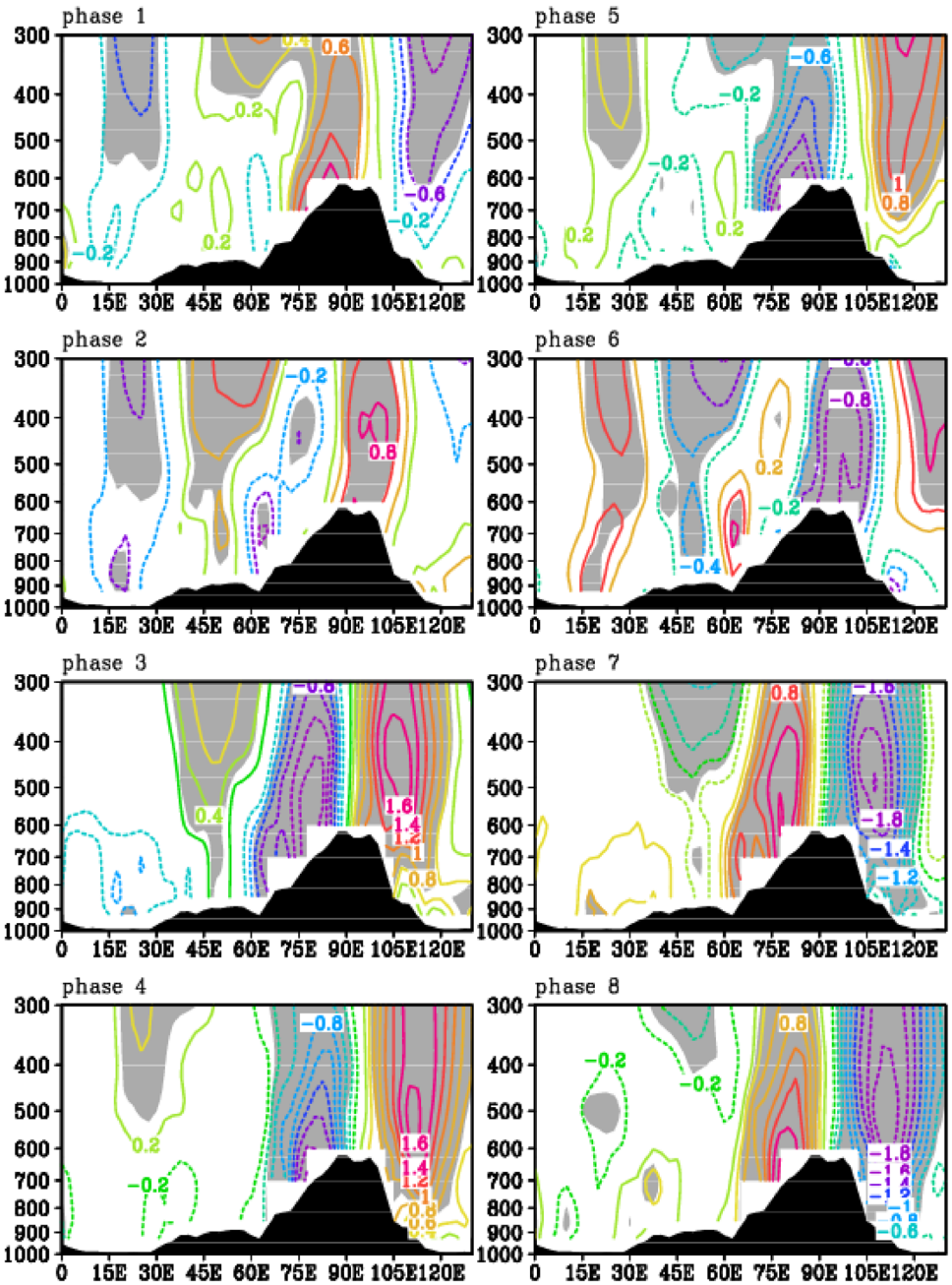


**Fig. 9** Height-longitudinal cross-sections of composites of 10–20-day filtered potential pseudo-equivalent temperature ($\theta_{se}$) (units: K) averaged between 30°N–40°N for eight QBWO phases. *Gray shadings* indicate the area with statistical significance exceeding 95% confidence level. The *black shadings* denote the topography of the Tibetan Plateau

The heating depresses the isobaric surface at 500 hPa, benefiting for the maintenance and eastward movement of TPVs. Thus, the anomalous circulations and the heating fields in positive phases cause a favorable situation for the TPVs to move off the Tibetan Plateau. As a result, most of the moving-off TPVs are found in positive phases.

## 5 Summary and discussion

In this study we investigated the relationship between the 10–20-day QBWO and the TPVs moving off the Tibetan Plateau during May–August of 1998–2012, and further revealed the mechanisms of the effect of 10–20-day QBWO on the moving-off TPVs. The main results are as follows:

1. Significant 10–20-day QBWO is revealed by the power spectrum of 500 hPa vorticity averaged over ETP. 77% of the moving-off TPVs are found in positive QBWO phases. The frequency for the locations of TPVs appearing in the positive phases are much higher than those in negative phases, with the maximum frequency in phase 3 when strongest QBWO occurs, and the loca-

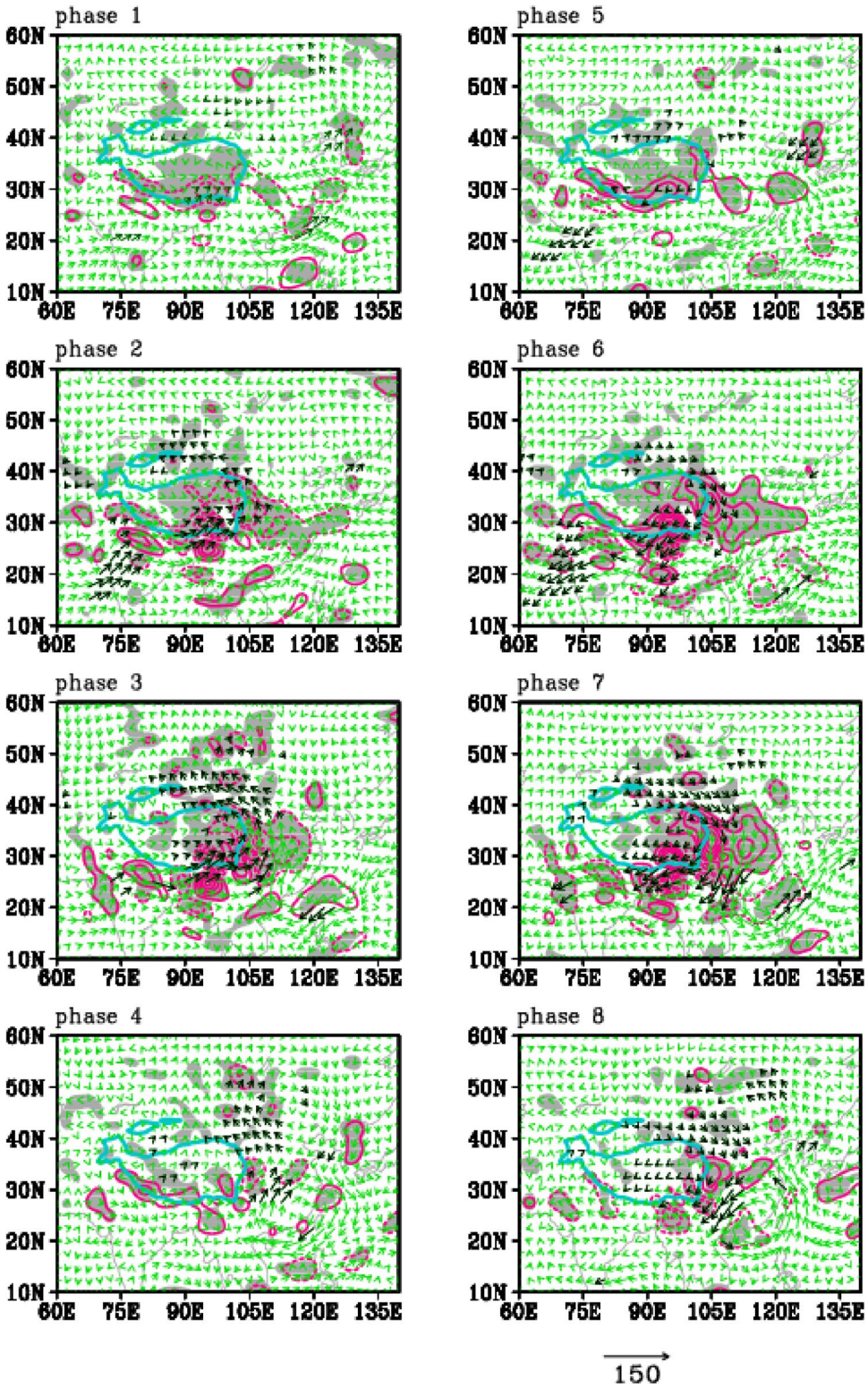


**Fig. 10** Same as Fig. 7, but for vertically integrated water vapor flux (vectors; unit: kg $m^{-1}$ $s^{-1}$) and water vapor flux divergence (contours; unit: $10^{-5}$ kg $m^{-2}$ $s^{-1}$). Water vapor flux and water vapor flux divergence with statistical significance exceeding 95% confidence level are expressed by *black-colored vectors* and *shadings*, respectively

tions of TPVs stretch eastward, indicating the eastward movement of TPVs.

2. *E* vector at 500 hPa is calculated to investigate the relationship between the propagation of the low frequency energy of 10–20-day QBWO and the eastward movement of TPVs. The positive zonal component of *E* vectors is located over eastern Tibetan Plateau, and the positive and negative meridional components are located to the north and south of about 34°N over eastern Tibetan Plateau, respectively. This distribution of

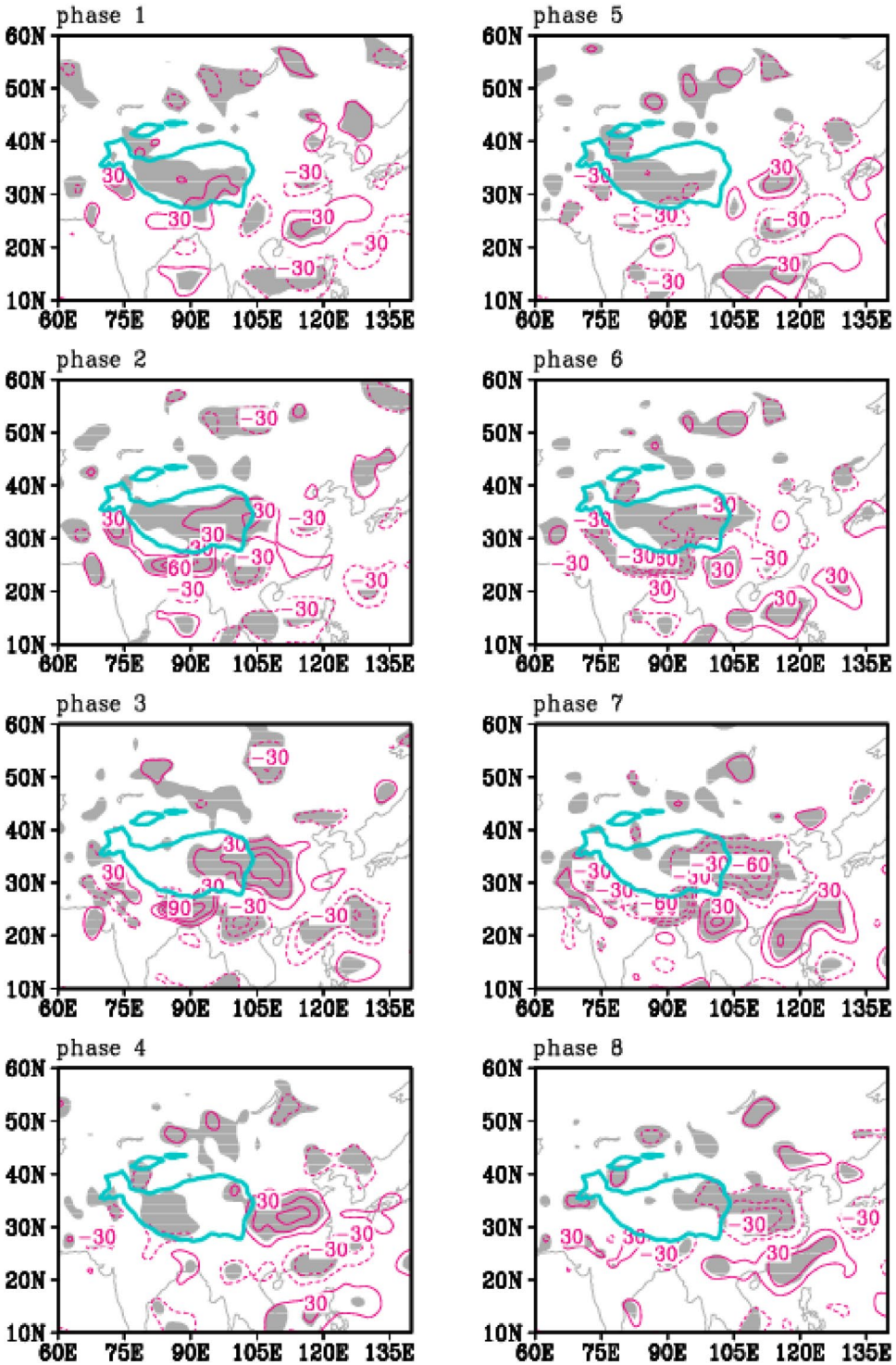


**Fig. 11** Same as Fig. 7, but for vertically integrated atmospheric apparent moisture sink (<$Q_2$>) (unit: K day$^{-1}$)

*E* vectors coincides well with the trajectories of the moving-off TPVs, which shift eastward in line with the positive zonal component of *E* vectors, northward to the north of 34°N and southward to the south of 34°N in line with the positive and negative meridional components, respectively.

3. The moving-off TPVs are modulated by the circulations and thermodynamic fields of the 10–20-day QBWO. In the positive QBWO phases, at 500 hPa, negative geopotential height anomalies occupy the Tibetan Plateau, and anomalous cyclonic wind shear is found over ETP, which is in favor of the maintenance

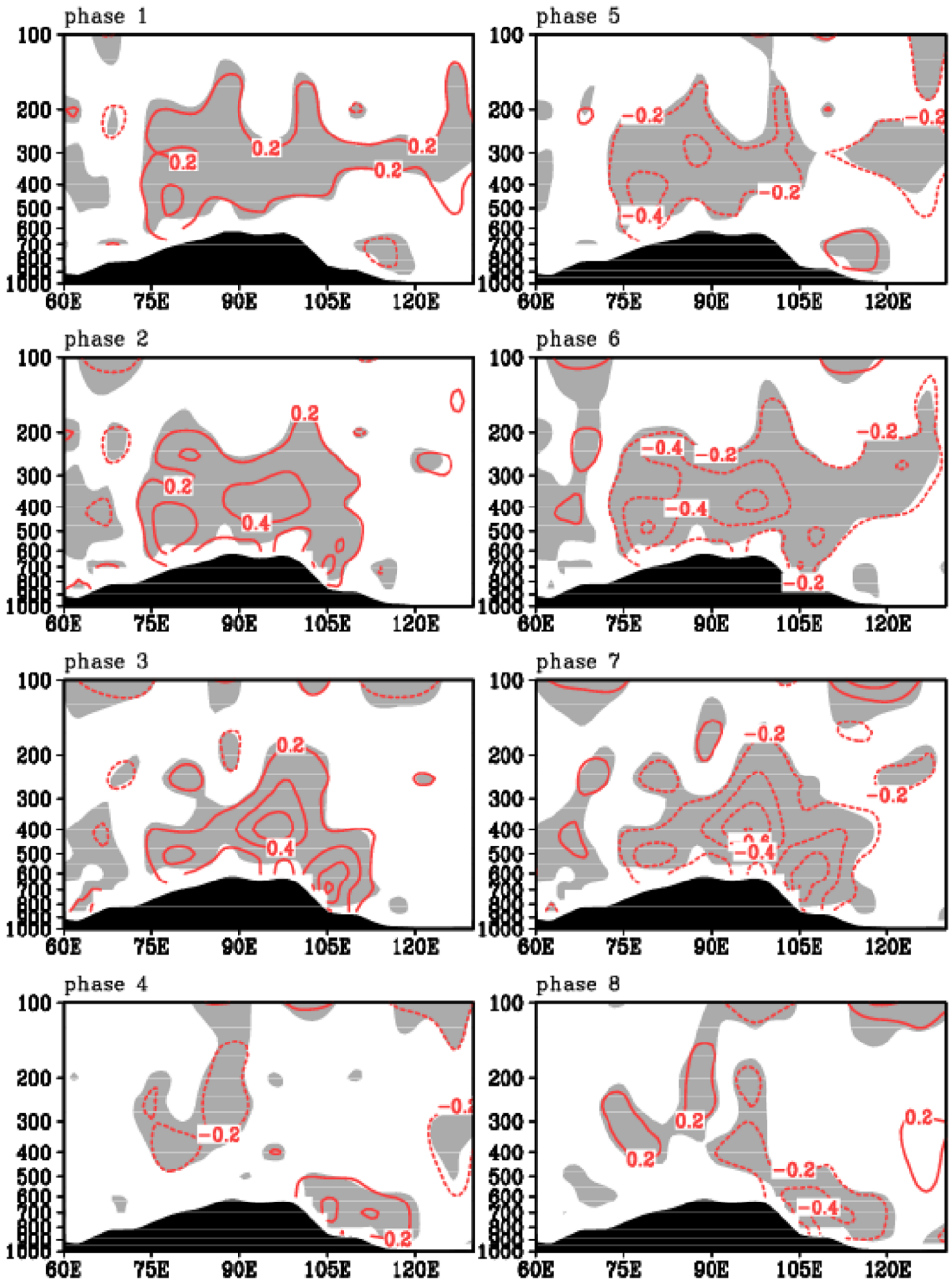


**Fig. 12** Same as Fig. 9, but for atmospheric heat source ($Q_1$) (unit: K day$^{-1}$)

and eastward movement of TPVs. At 200 hPa the anomalous jet stream over the northeast of the Tibetan Plateau and positive geopotential heights benefit for the upper-level divergence and ascending motion over ETP. In thermodynamic fields, the water vapor of QBWO converges over ETP in positive phases. The condensation latent heat related to the precipitation plays a major role in atmospheric heat source, which shifts eastward with the heating centers located at 400 hPa. The heating depresses the isobaric surface at 500 hPa, benefiting for the maintenance and eastward movement of TPVs.

It should be pointed out that, because the topography can affect the dynamic and thermodynamic processes on the atmosphere over the Tibetan Plateau, the topography is an important factor affecting the eastward movement of TPVs (Shen et al. 1986a; Dell'osso and; Chen 1986; Wang 1987). Compared to the QBWO modulation, the role played by the topography in the moving-off TPVs need to be investigated through numerical experiments in the future. In addition, the results in the present study show that the QBWO of circulation may be related with anomalous circulations from higher latitudes originated from central Asia, whereas the water vapor transport associated with the QBWO seems to

be from the Arabian Sea. Which one is dominant or if there is a phase-lock between circulations originated from higher latitudes and water vapor coming from the tropical ocean are not dealt with in the present study. Anyway, the origination of the QBWO around the Tibetan Plateau and the effects of the systems from lower and higher latitudes on the QBWO are needed for further investigation.

**Acknowledgements** The authors are very grateful to the constructive comments from anonymous reviewers. The observational data are provided by the information center of Chinese Academy of Meteorological Sciences, and NCEP/NCAR Reanalysis data by the NOAA/OAR/ESRL PSD, Boulder, Colorado, USA, from their Web site at http://www.esrl.noaa.gov/psd/. The *Yearbooks of Tibetan Plateau Vortex and Shear Line* accomplished by the Institute of Plateau Meteorology, CMA from 1998 to 2012 are referred in selecting the TPVs. This work is supported by the China National 973 Project (2015CB453203), National Key Research and Development Program (No. 2016YFA0601504, 2016YFA0600602), the National Natural Science Foundation of China (Grant Nos. 41405054, 41661144017, and 41275050), the Basic Scientific Research and Operation Foundation of CAMS (Nos. 2015Z001, 2016Y001 and 2014R008), and the Special Fund for Tibetan Plateau Research (GYHY201406001).

## References

Chen BM, Qian ZA, Zhang LS (1996) Numerical simulation of formation and development of vortices over the Qinghai-Xizang Plateau in summer. Chin. J Atmos Sci 20:491–502 (**in Chinese**)

Dell'Osso L, Chen SJ (1986) Numerical experiments on the genesis of vortices over the Qinghai-Xizang Plateau. Tellus 38(A):235–250

Ding ZY, Lu JN (1990) A numerical experiment on the eastward movement of a Qinghai-Xizang Plateau low vortex. J Nanjing Ins Meteor 13:426–431 (**in Chinese**)

Duchon CE (1979) Lanczos filtering in one and two dimensions. J Appl Meteor 18:1016–1022

Gao WL, Yu SH (2007) Analyses on mean circulation field of the plateau low vortex moving out of the Tibetan Plateau. Plateau Meteor 26:206–212 (**in Chinese**)

Gu QY, Shi R, Xu HM (2010) Comparison analysis of the circulation characteristics of plateau vortex moving out of and not out of the plateau. Meteor Mon 36:7–15 (**in Chinese**)

Guo MZ (1986) General investigation of the moving eastward Lows over Qinghai-Xizang Plateau. Plateau Meteor 5:184–188 (**in Chinese**)

Hoskins BJ, James IN, White GH (1983) The shape, propagation and mean-flow interaction of large scale weather system. J Atmos Sci 40:1595–1612

Jia XL, Yang S (2013) Impact of the quasi-biweekly oscillation over the western North Pacific on East Asian subtropical monsoon during early summer. J Geophys Res Atmos 118:4421–4434

Kalnay E et al (1996) The NCEP/NCAR 40-year reanalysis project. Bull Am Meteor Soc 77:437–470

Lhasa group for Tibetan Plateau meteorology research (1981) Research of 500 hPa vortices and shear lines over the Tibetan Plateau in summer. Science Press, Beijing (**in Chinese**)

Li GP (2002) The Tibetan Plateau dynamic meteorology. China Meteorological Press, Beijing (**in Chinese**)

Li GP, Zhao BJ (2002) A dynamical study of the role of surface sensible heating in the structure and intensification of the Tibetan Plateau vortices. Chin J Atmos Sci 26:519–525 (**in Chinese**)

Li L, Zhang RH, Wen M (2011) Diagnostic analysis of the evolution mechanism for a vortex over the Tibetan Plateau in June 2008. Adv Atmos Sci 28:797–808

Li L, Zhang RH, Wen M (2014a) Effect of the atmospheric heat source on the development and eastward movement of the Tibetan Plateau vortices. Tellus A 66:24451. doi:10.3402/tellusa.v66.24451

Li L, Zhang RH, Wen M (2014b) Diurnal variation in the occurrence frequency of the Tibetan Plateau vortices. Meteor Atmos Phys 125:135–144

Liu FM, Fu MJ (1985) A study on the moving eastward Lows over Qinghai-Xizang Plateau. Plateau Meteor 5:125–134 (**in Chinese**)

Luo SW (1992) Study on some kinds of weather systems over and around the Qinghai-Xizang Plateau. China Meteorological Press, Beijing (**in Chinese**)

Luo SW, Yang Y, Lu SH (1991) Diagnostic analyses of a summer vortex over Qinghai-Xizang Plateau for 29–30 June 1979. Plateau Meteor 10:1–11 (**in Chinese**)

Luo SW, He ML, Liu XD (1994) Study on the vortex of the Qinghai-Xizang (Tibet) Plateau in summer. Sci China Ser B37:601–612

Qiao QM, Zhang YG (1994) Synoptic meteorology of the Tibetan Plateau and its effect on the near areas. China Meteorological Press, Beijing (**in Chinese**)

Rasmusson EM (1968) Atmospheric water vapor transport and the water balance of north America II. Large scale water balance investigations. Mon Wea Rev 96720–96734

Shen RJ, Reiter ER, Bresch JF (1986a) Numerical Simulation of the Development of Vortices over the Qinghai-Xizang (Tibet) Plateau. Meteor Atmos Phys 35:70–95

Shen RJ, Reiter ER, Bresch JF (1986b) Some aspects of the effects of sensible heating on the development of summer weather system over the Qinghai-Xizang Plateau. J Atmos Sci 43:2241–2260

Sun GW, Chen BD (1994) Characteristic of the lows flocking with Tibet atmospheric low-frequency oscillation over the QinghaiXizang (Tibet) Plateau. Chin. J Atmos Sci 18:112–121 (**in Chinese**)

Wang B (1987) The development mechanism for Tibetan Plateau warm vortices. J Atmos Sci 44:2978–2994

Wang X, Li YQ, Yu SH, Jiang XW (2009) Statistical study on the plateau low vortex activities. Plateau Meteor 28:64–71 (**in Chinese**)

Wei W, Zhang R, Wen M, Yang S (2017) Relationship between the Asian westerly jet stream and summer rainfall over central Asia and North China: Roles of the Indian monsoon and the South Asian High. J Clim 30:537–552

Xu JJ, He JH (1993) The distribution of E vector about summer LFO and its related time mean flow. Acta Meteor Sin 51:103–110

Xuan SL, Zhang QY, Sun SQ (2011) Anomalous midsummer rainfall in Yangtze River-Huaihe River Valleys and its association with the East Asia westerly jet. Adv Atmos Sci 28:387–397

Yanai M, Steven E, Chu JH (1973) Determination of bulk properties of tropical cloud clusters from large-scale heat and moisture budgets. J Atmos Sci 30:611–627

Ye DZ, Gao YX (1979) The Tibetan Plateau meteorology. Science Press, Beijing (**in Chinese**)

Yu SH (2002) Water vapor imagery of vortex moving process over Qinghai-Xizang Plateau. Plateau Meteor 21:199–204 (**in Chinese**)

Yu SH, Gao WL, Gu QY (2007) The middle-upper circulation analyses of the Plateau low vortex moving out of Plateau and influencing flood in east China in recent years. Plateau Meteor 26:466–475 (**in Chinese**)

Yu SH, Gao WL, Xiao DX, Peng J (2016) Observational facts regarding the joint activities of the southwest vortex and plateau vortex after its departure from the Tibetan Plateau. Adv Atmos Sci 33:34–46

Zhang PF, Li GP, Fu XH, Liu YM, Li LF (2014) Clustering of Tibetan Plateau vortices by 10–30-day intraseasonal oscillation. Mon Wea Rev 142:290–300

Zhou SW, Zhang RH (2009) Comparison of NCEP/NCAR reanalysis data and radiosonde data about temperature and geopotential height of upper air over the Tibetan Plateau. Clim. Environ Res 14:284–292 (**in Chinese**)